Review Article

Dental Hard Tissue Ablation with Laser Irradiation

Al-Jedani S[1], Al-Hadeethi Y[1,2]*, Ansari MS[3] and Razvi MAN[1]

[1]Physics Department, King Abdulaziz University, Saudi Arabia

[2]Lithography in Devices Fabrication and Development Research Group, King Abdulaziz University, Saudi Arabia

[3]Centre of Nanotechnology, King Abdulaziz University, Saudi Arabia

*Corresponding author: Yas Al-Hadeethi, Physics Department, King Abdulaziz University, Saudi Arabia

Abstract

This article reviews work on the laser dental hard tissue ablation. Results obtained by irradiating dentine and enamel using Nd:YAG laser irradiation are presented. Results were analyzed using SEM, optical microscopy, LIBS and Micro Raman Spectroscopy. Dentine and enamel ablation, crater depth measurements, morphology of processed cavities in dentin and enamel, the appropriate set of laser parameters to ensure surfaces with no evidence of melting, carbonization or micro-cracks are investigated. Micro Raman spectra were utilized for hard tissue ablation studies. The EDS quantitative analyses are presented to study the atomic percentage of carbon in tandem with an increase in laser energy density for enamel and dentin. EDS quantitative analysis are used to Ca/P ratio as influenced by the laser energy density increase for enamel and dentin.

Abbreviations

CW: Continuous Wave; FDA: Food and Drug Administration; FESEM: Field Emission Scanning Electron Microscopy; LIBS: Laser Induced Breakdown Spectroscopy; EDS: Energy Dispersive X-ray Spectroscopy; IR: Infra-red

Introduction

Soon after its advent, laser was used as a tool for scientific research. During the 1960s and 1970s, there was a rapid advancement with the development of different types of lasers [1]. Laser ablation is implemented in several scientific and technological fields. It has become a dominant technology for such applications as production of nano-materials, deposition of dielectric films, micromachining and chemical analysis. It is an active subject of theoretical and experimental investigation, which has been widely studied for its large applications ranging from basic physics investigations to medical and technical applications. Laser ablation of biomaterials including human teeth is of currently growing interests. Laser applications in dentistry started directly soon thereafter its advent. Initially, laser operation modes were CW with non-contact delivery, which were found to be too hot for practical dental use. One of these early lasers that were proposed for dentistry applications was CO_2 laser [2]. It was developed repeatedly and had a limited use for ablation of soft tissue by oral surgeons. Laser medical technology underwent significant development in the early 1980s since the appearance of short laser pulse durations and fiber optic contact delivery [2]. Laser devices found their way to the dental industry fairly rapidly, but along with concerns regarding heat transfer and, consequently, possible damage to the tooth [3].

Since 1990s, lasers began to be used in dental procedures [4] with success [5,6]. The breakthroughs involved better control over the delivery of laser light in both the temporal and spatial characteristics. The major competitors in this market have been utilizing either Nd:YAG, with wavelength (λ) at 1064nm, Er:YAG, with wavelength at 2940nm, and Er,Cr:YSGG, with wavelength at 2783nm. Dental lasers have had a huge growth in practical dental applications [2]. Nowadays, dental lasers are divided into three basic types: soft tissue laser, hard tissue laser, and non-surgical laser such as diagnostic composite and photo-disinfection. Laser dental applications have several advantages:

(I) They limit hemorrhage in soft tissue [7].

(II) They can be used in the treatment of soft and hard tissue, such as Er, Cr:YSGG and Er:YAG. They were approved by the FDA clearance for both hard and soft tissue applications [8];

(iii) They have unique properties, such as monochromaticity - a property that makes laser to have impact on a specific type of tissue or compounds without interfering with the rest of the compounds [8].

(iv) Their high energy which facilitate using laser radiation as sterilizing tool, by killing most of the bacteria [9].

(v) Laser devices make little or no noise compared to conventional tools, giving patients greater psychological comfort [10].

(vi) They reduce the feeling of pain, thereby reducing the need to use anesthetic [10].

However, lasers have the following disadvantages in dentistry:

(i) Laser ablation of calcified tissue can lead to irreversible harm of fractures and fissures, owing to the fact that hard tissue is susceptible to both shear and compressive stresses [11].

(ii) Temperatures may rise in the pulpal chamber during laser irradiation [12].

(iii) Lasers cannot be used on teeth with fillings already in place [13].

(iv) Laser devices can be more expensive compared to hand drill [13].

Despite the dangers associated with the use of lasers to ablate hard tissue, they are still attractive since they offer the potential for rapid, precise, and accurate operation with minimal thermal and mechanical damage to surrounding tissue [11].

On the other hand, laser risks and adverse effects should be addressed. When evaluating any product such as lasers for use in
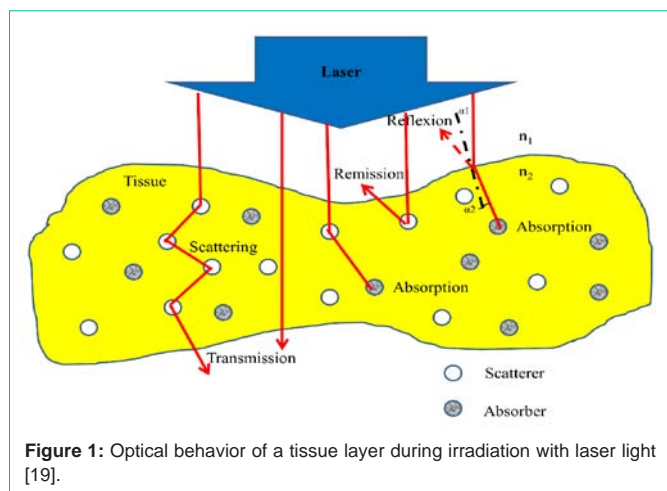
Figure 1: Optical behavior of a tissue layer during irradiation with laser light [19].

Table 1: Laser tissue Interaction Parameters.

Tissue Properties		Laser Properties
Optical Properties	**Thermal Properties**	
Reflection Absorption Scattering Transmission	Heat conduction Heat capacity	Wavelength Exposure time Power and energy density Spot size Operation mode

patient's treatment, their safety, efficacy and effectiveness have to be considered and investigated [14]. Safety requires that collateral damage be assessed histologically at multiple points and can be verified from being within the allowable limits [14]. This evaluation includes consideration of the healing outcome in terms of the pre-operative state and any lasting and undesirable damage along with clinical benefit. The risk-benefit proportion must be small, with significant capabilities of interest to the patient [14]. The risk of eye damage is the main physical risk in laser treatment. While this had never been reported, the risk of possible eye damage should be considered, especially when using invisible radiation. As a result, the patient should put on appropriate protective goggles [15]. Furthermore, there are many challenges facing laser dentistry. For instance, there are still many areas of dentistry where only conventional treatments can be performed effectively. As an example, laser dentistry cannot be used to penetrate teeth with previous fillings or in patients who have cavities between teeth. Moreover, treatment cost is significantly higher compared to conventional therapies. Another challenge is the fact that some lasers such as Nd:YAG, with power levels of 1-3 W, elevate temperatures in the pulp chamber to a sufficient degree that cause at least localized pulpal inflammation and possibly irreversible damage to pulpal tissue [12]. The enamel layer is damaged in the course of time, pre disposing the patient to dental caries, breakage and dentin sensitivity [16]. Accordingly, there is a need to develop lasers capable of overcoming the aforementioned problems. Dentin and pulp may be injured not only by dental caries but also from procedures necessary for the repair of lesions involving dental hard tissue [17]. We expect that laser ablation is not going to injure dentin and pulp if laser thermal effects are avoided. Laser ablation leads to the escalation of vapor if laser is used on amalgam (dental restorative material). It may be prudent for clinicians to polish amalgam restorations after laser is used to minimize any inadvertent damage to these restorations [18].

Moreover, conventional dental treatment is always accompanied by worry, fear, pain and discomfort. Accordingly, it is important to look for other dental treatment approaches to avoid the aforementioned discomforts. Thus, it is necessary to invent better approaches, which can attain better treatment results.

Laser tissue interaction

To select a suitable laser system for the medical applications, it is necessary to understand its biological effect on tissue. Therefore, for any laser to have an effect on living tissue, the tissue molecules must first absorb it. If the energy is reflected from the surface of a tissue, or if it is completely transmitted through a tissue, then no biological effect would result [19]. When the laser beam interacts with tissue, several processes may occur such as scattering by changing their direction of flight according to the probability function known as the anisotropy factor, or absorbed by tissue molecules that would lead to molecules excitation by an electronic transition [19]. There is another possibility, where about 4–10% of laser beam might be refracted due to the refractive index change and according to the angle of incidence. Also, after laser beam penetrating the tissue initially it refracted, according to Snell's law, which provides: "that photons entering a medium with a higher refractive index are refracted towards the vertical axis to the surface", (Figure 1), summarizes these processes [19].

Laser tissue interaction parameters: To design a pulsed laser system for tissue ablation purpose, first several irradiation parameters must be selected. Typically, one selects the wavelength first. Unfortunately, it is usually the case that not all parameters can be selected independently [20]. Laser-tissue interactions can be affected by many parameters such as, the target tissue characteristics (optical and thermal properties), also by laser type and settings (wavelength, pulse duration, energy density, and exposure time). The parameters are summarized in (Table 1). The previous interaction parameters share single common information that is the characteristic energy density that ranges from approximately 1 J/cm^2 to 1000 J/cm^2. So the main parameter that controls the laser tissue interaction is the duration of the laser exposure [21]. A summery map of the relationship between the main classifications of laser-tissue interactions, and the most important interaction parameters (energy density, exposure time and power density) is shown in (Figure 2) [22].
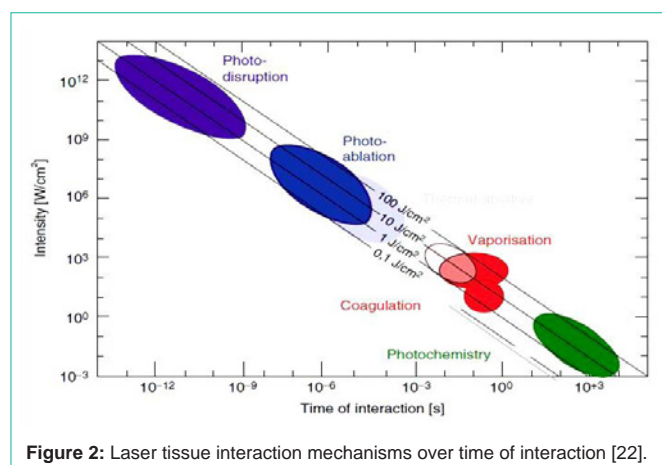

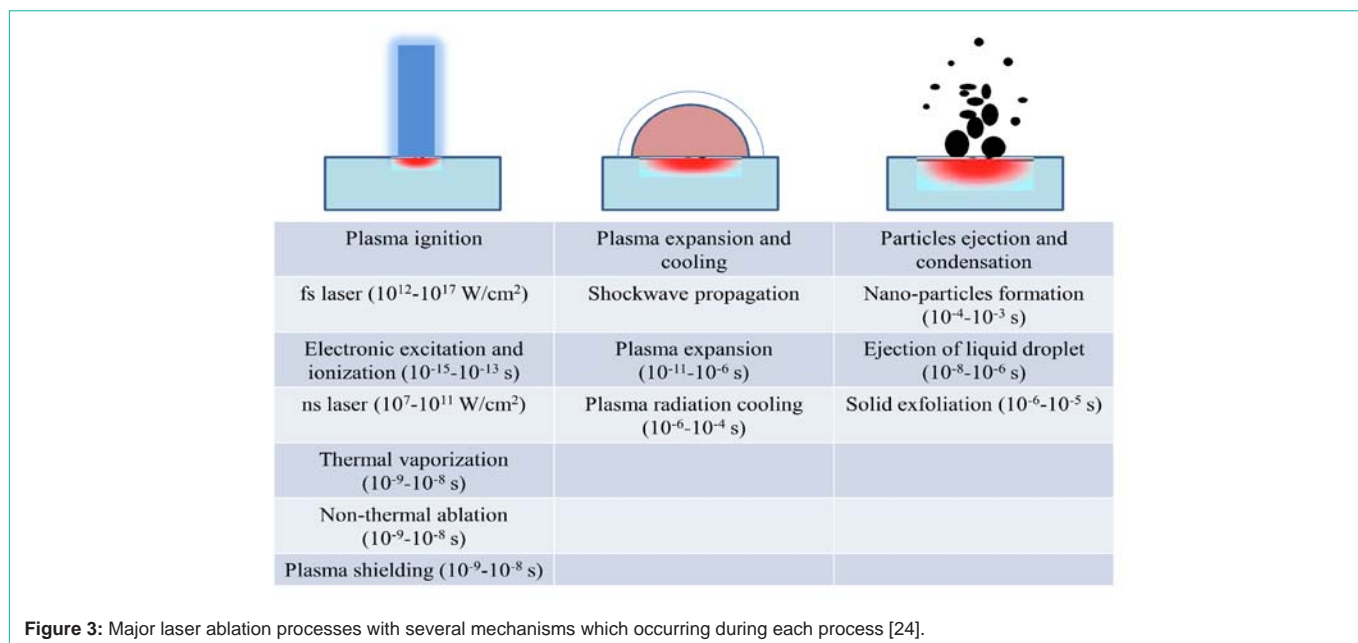**Figure 2:** Laser tissue interaction mechanisms over time of interaction [22].

Figure 3: Major laser ablation processes with several mechanisms which occurring during each process [24].

Laser ablation

Merriam-Webster dictionary defined the ablation as "loss of a part by melting or vaporization". In order for ablation to occur, energy absorption is needed. The energy can be provided in the form of electrical discharges like a spark or in the form of light as a laser. The laser ablation can be defined as follows: "the process of removing material by using laser beam energy, either by melting, fusion, sublimation, ionization, erosion, and/or explosion". Laser ablation produces a gaseous vapor, plasma, and fine particles. The laser-material interaction can be divides into two cases depending on the energy density. First, at low laser energy density, the material is heated by the absorbed laser energy and evaporates or sublimates. Second, at high laser energy density, the material is converted to plasma, and this often occurs by using a pulsed laser. Usually, laser ablation refers to ablated material with a pulsed laser, but it is possible to ablate material with a continuous wave laser beam if the energy density was high enough [23].

Fundamental ablation processes: Laser ablation is governed by a variety of distinguished nonlinear mechanisms. The moment that the pulsed laser beam illuminates the sample, plasma formation may take place, which leads to remove a mass from the sample surface in the form of electrons, ions, atoms, molecules, clusters, and particles. Each of the processes is separated in time and space. An understanding of the basic mechanisms involved in each of these processes is critical for efficient laser-tissue interaction, and to removing mass in the right shape for analysis [24].

Laser ablation steps are divided into the following three major processes:

1. Breaking the material bond and plasma ignition.

2. Plasma expanded and cooling.

3. Particle ejection and condensation.

These laser ablation steps occurring over several orders of magnitude in time, beginning with electronic absorption of laser beam energy (10-15 second) to particle condensation (10-3 second) after the laser pulse is completed [24]. Summary of these three steps are shows in (Figure 3). During the plasma ignition process, the plasma properties and mechanisms are strongly depending on the laser intensity and pulse duration. For a nanosecond laser pulse with intensity less than $108 W/cm^2$, the predominant mechanism is thermal vaporization, the temperature of the solid surface increases, and a well-defined phase transition occurs, from solid to liquid, liquid to vapor, and vapor to plasma [24].

Photomechanical induced ablation: When short-pulsed laser interacts with the material, specifically pulse duration in nanosecond region and the laser produces heat, which produces explosive behavior in the affected zone (laser-material interaction area). Because of the sudden rise in temperature, the sample experiences an impulsive mechanical excitation that creates acoustic and shock waves [25]. Removing the material using these mechanisms is denoted as photo-mechanically induced ablation. However, the zone, which surrounds the ablated region, is exposed to photomechanical collateral damages in the form of fractures and cracks. For the sake of exciting stress waves that are capable of introducing physical damage, the laser pulse length (τp) has to be shorter than the acoustic diffusion time (τa), which is needed to insure propagation of stress waves out of the laser-affected zone. The stress wave propagates through a medium at the speed of sound (σ). Therefore, the acoustic diffusion time can be expressed as:

$$\tau a = \delta/\sigma \ (1)$$

The optical penetration depth (δ) of the laser beam is the depth at which the energy of the collimated laser has been reduced to 37 % of the incident energy. This depth is related to the absorption coefficient (μa) as:

$$\delta(\lambda) = 1/\mu a \ (\lambda) \ (2)$$

Laser pulse durations, which are shorter than τa are able to

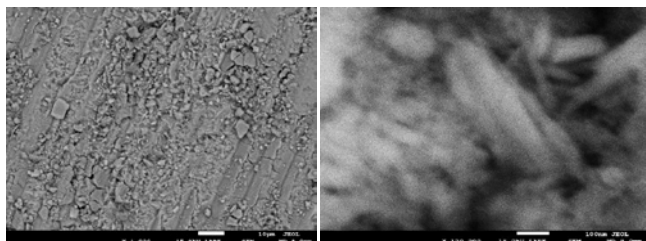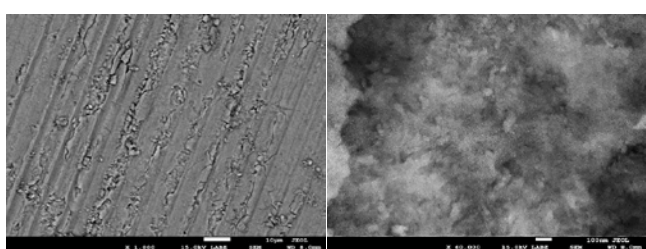**Figure 4:** SEM image of dentin surfaces after cut it with diamond disc.

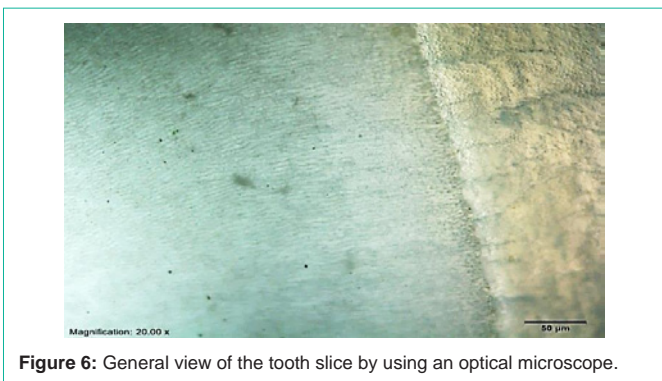**Figure 5:** SEM image of enamel surfaces after cut it with diamond disc.

Figure 6: General view of the tooth slice by using an optical microscope.

introduce mechanical energy within the optically affected zone in the form of, stress waves. The afore mentioned condition is referred to as the stress confinement, and is determined by the following criteria [25].

$$\tau p < \tau a \quad (3)$$

The differentiation between plasma-induced ablation and photo-disruption is emphasized and properly substantiated.

Nanosecond laser ablation: The ablation in the nanosecond region is completely dominated by hydrodynamics, where the plasma plays a significant role in nanosecond ablation. Beginning with the laser material surface interaction, a low-density plasma corona would form in front of the target surface. With the plasma is formed, the laser beam interacts with the plasma and it would absorbed in the plasma corona at the critical surface. After that, the energy will be transferred inside target surface by electronic-thermal conduction [26]. The material particles are constantly removed from the target or ablation surface, while the plasma is fed by laser beam energy and expands in a vacuum. A shock wave would form behind the ablation surface and expands inside target material, which is formed because of momentum conservation. The shock wave spreading inside target material and lead to pressure formation that compressed the material. The shock wave front and the ablation front move inside the material

that cause photo-disruption. The shock is also a very effective factor, which produces further ablation of material. However, measuring the ablation depth can be difficult because of the rough ablated surface [27]. During the photo-disruption, mechanical forces split the tissue. Whereas plasma induced, ablation is spatially confined to the breakdown region. For pulse durations in the nanosecond range, the spatial extent of the mechanical effects has been already of the order of millimeters even at the very threshold of breakdown. Shock wave and cavitation affects the propagate into adjacent tissue, thus limiting the localizability of the interaction zone [26].

Results and Discussion

This section includes a full description of the tooth surface qualitative evaluation as the normal histology, and the morphological changes of enamel and dentin after Nd:YAG laser treatment. It also provides quantitative evaluation of the ablation behaviours using the nanosecond pulse duration Nd:YAG laser at wavelength 1064 nm. Furthermore, it presents the laser effects on enamel and dentin surfaces by using different energy densities and number of pulses. Results of this article are compared to works of other researchers whenever necessary.

Enamel and dentin morphological analysis

The teeth were sectioned into slices, after that, FESEM images were taken for the sliced surface to understand the morphology evolution after laser treatment. Results can be seen in (Figure 4 and Figure 5). FESEM images show smear layer. It is a layer of micro and nano-crystalline, which is formed during cutting process. (Figure 4 and Figure 5) show nano-crystalline structures of dentin and enamel surface respectively following cutting with diamond disk. The smear layer might act as an obstacle in the field of vision and imaging. It was completely removed by using polishing method. After that, tooth histology was observed by optical microscope as seen in (Figure 6 and Figure 7). In (Figure 6) we can see the boundary between the enamel and the underlying dentin that is called a dental - enamel junction. At the light microscopic level, the characteristic arrangement of crystals gives rise to rod core and inter-rod substance. In the cross section, enamel rods demonstrate a characteristic key hole or fish scale pattern as seen in (Figure 6 and Figure 7). These patterns are due to the differences in orientation of the enamel crystallites, in the rod core, apatite crystals are oriented parallel to the long axis of the rod. In inter-rod substance, the crystals have an oblique angulation. The rod sheath is due to an increase in space, and as a result an increase in water and protein [28]. As shown (Figure 7), we can see dental tubules and enamel rods very clearly. The normal enamel surface
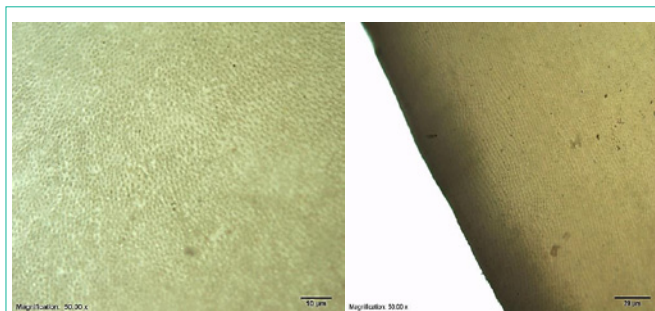

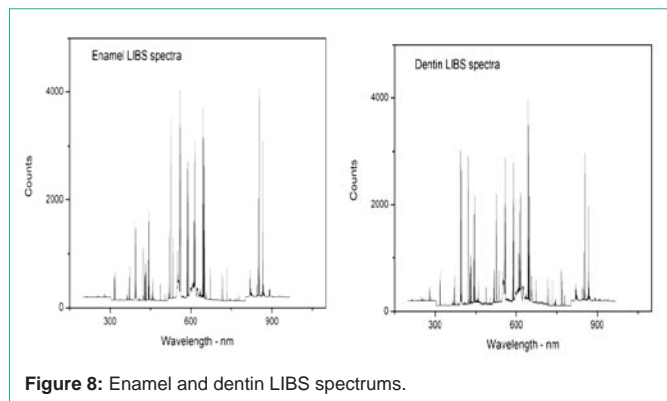**Figure 7:** Optical microscope images for enamel and dentin.

Figure 8: Enamel and dentin LIBS spectrums.

of sound teeth presents characteristic depressions and enamel rod. In (Figure 6 and Figure 7) the surface of the sound dentin shows numerous parallel dentin tubules. In addition, the dentinal tubules are structures that span the entire thickness of dentin, they radiate outward through the dentin from the pulp to the exterior enamel border.

Laser ablation characteristics

Ablation thresholds determination: To determine the ablation thresholds (J/cm^2) of dentin and enamel, a multi-pulse irradiation of the samples at a variable laser energy density (J/cm^2) was performed. In this work, ablation threshold is defined by the appearance of minimal intensity of calcium line by using LIBS. The ablation threshold is generally defined as the minimum energy that atom needs to escape from the material [29]. Dentin and enamel samples were ablated with Nd:YAG laser operating at 1064nm, with a 5ns pulse duration, and 1Hz repetition rates. When a high power pulse-laser beam is incident onto the target, it leads to local heating and evaporation of the sample materials. The ablated materials expands and forms the plasma plume front in the ambient atmosphere [30]. From this point, there is a relationship between the plasma intensity and the ablated material. Using higher laser energy lead to obtained highest plasma intensity and ablated material. One of the good methods to study this relationship is by using LIBS. Using LIBS allows defining both the element in the sample and plasma intensity. The intensity of a given emission line is proportional to the number density of emitters which, in turn, is proportional to the concentration of the emitter in the irradiated sample. Therefore, the emission intensity is linearly correlated to the concentration of a given species in the sample [31]. The integrated peak area of the calcium line at 393.3, 396.8, 422.6, 442.5, and 445,4nm were plotted for different energy densities in (Figure 8). As expected, an increase in emission intensity with the increased incident energy density. We noticed that ablation thresholds for enamel and dentin were close to plasma formation thresholds. The line spectrum of calcium appears clearly at an energy density of 3.5J/cm² for both enamel and dentin. The relationship between integrated peak areas of calcium line and energy density were examined by a curve fitting analysis of the experimental data for enamel and dentin. The best curve fitting for enamel results was exponential fit; while the best curve fitting for dentin results was the linear fit for all calcium lines. After selecting the best equation from curve fitting, the interrupt points with X-axis were determined for all curves. The ablation thresholds of Nd:YAG lasers in enamel and
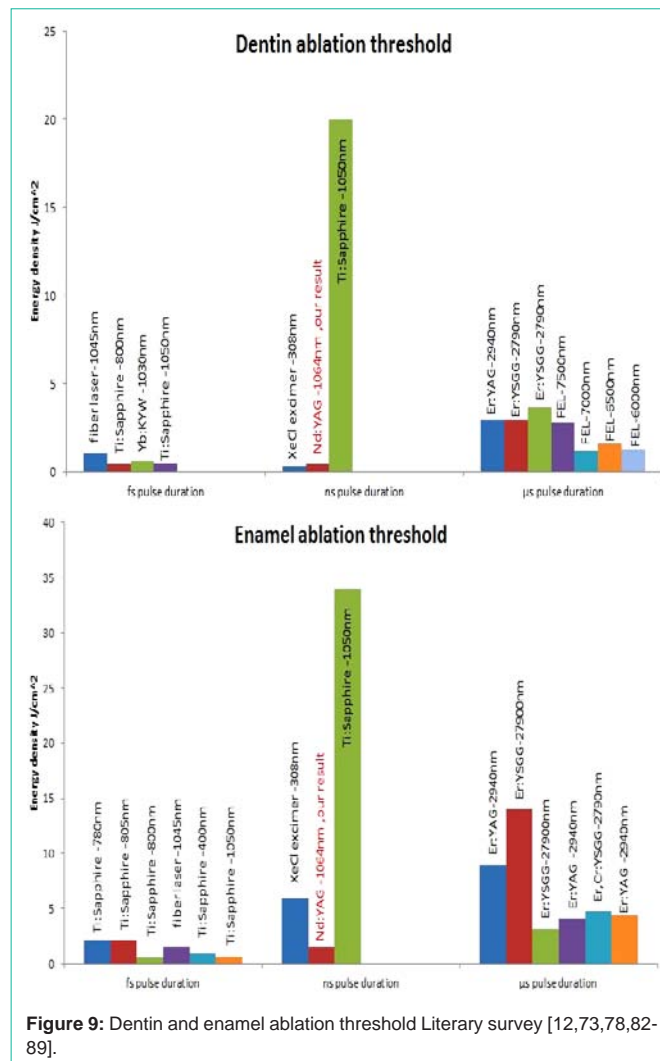

Figure 9: Dentin and enamel ablation threshold Literary survey [12,73,78,82-89].

dentin were found to be 1.37, and 0.6 J/cm², respectively as reported by authors somewhere else [32]. Enamel has a higher threshold than those of dentin. This may be imputed to the following reasons: Enamel is composed by volume of 85% mineral 12% water, and 3% organic proteins. Dentin is composed by volume of 47% mineral, 33% protein mostly collagen, and 20% water. Dentin has a higher water content and less mineral density than enamel [33,34]. Using a high energy density to ablated dentin must be excluded since dentin contains organic materials and nerves that make it very sensitive as getting near to the pulp [28]. Moreover, tooth dentin has abundant dentinal tubules that make it as porous as sponge. In addition, the tubules provide the tissue with elasticity and relatively low hardness that would then result in the dentin's lower ablation threshold with lasers. Interestingly the ablation threshold values of this reported work were found to be lower than given in previously published work (Figure 9) and this is attributed to using shorter pulse duration [35]. Laser ablation characteristics depend on both the physical properties of the target material and the parameters of the laser radiation. Normally, the object under study is pre-determined and the main problem lies in the selection of the laser parameters for the effective ablation (wavelength, intensity, pulse duration, and pulse repetition rate) [35].
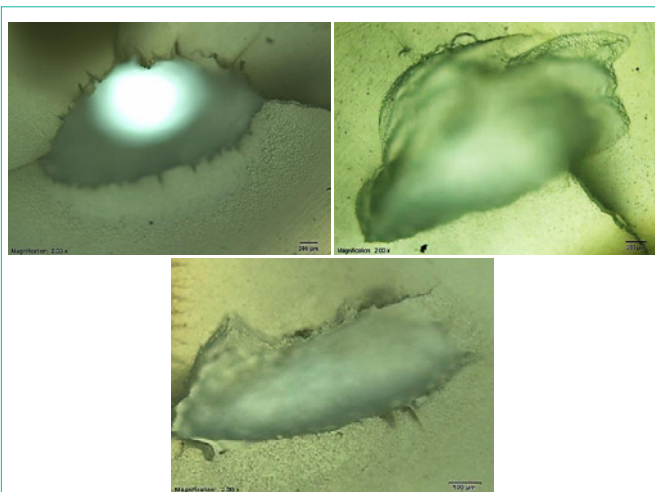
Figure 10: Optical microscope images of the crater in dentin by using energy densities of 17.08, 11.18, and 5.6 J/cm².
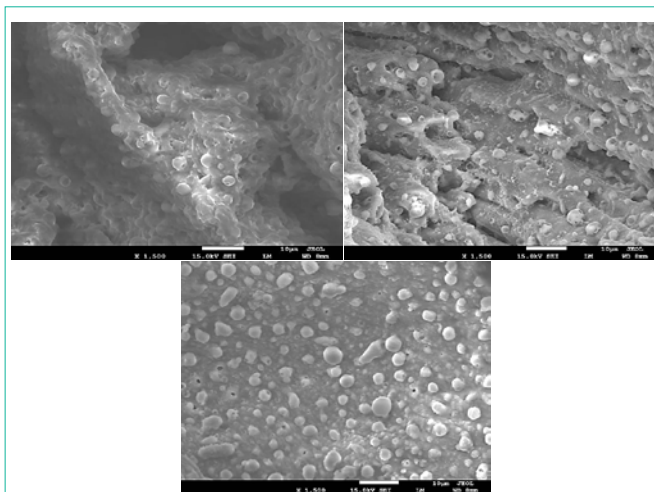
Figure 12: Dentin surface after irradiated with laser energy densities of 17.08,11.18, and 5.6 J/cm².

Figure 11: Optical microscope images of the crater in enamel by using energy densities of 17.08, 11.18, and 5.6J/cm².

Enamel and dentin morphological changes

Morphological changes were studied, for both enamel and dentin after laser irradiation by using two techniques; the optical microscope to give a general view of the craters and the FESEM to study the microscopic changes in enamel and dentin surface.

Optical microscope results: Using an optical microscope allows getting a general view of ablation surface and cracks. The general view of craters in dentin that were obtained using energy densities of 17.08, 11.18, and 5.6 J/cm² and 300 pulses for each crater is shown in (Figure 10). The surrounding area showed very clear melting with some cracks. With increasing energy density, the melting and cracks were increasing. The crater depth also increases by increasing the energy density. Unlike dentin, enamel has not been affected by laser irradiation, though, same energy densities that were used for dentin (17.08, 11.18, and 5.6 J/cm²) and the same number of shot (300 shots) as shown in (Figure 11). In enamel, melting at the edge of crater and a non-uniform surface of ablation has been observed. The crater's depth was found to increase with the increase of energy density and

the ablation surface was uniform. By comparing enamel crater to dentin crater, it was noticed that dentin has deepest crater even when using the same experimental setup.

Dentin SEM results: By using fixed number of (300shots), and by using different energy densities ranging from 17.08, 11.18, to 5.6 J/cm², the results of (Figure 12) were obtained. All samples that were irradiated with Nd:YAG laser show significant morphological changes. Samples that were exposed to a high number of shorts or a higher energy density showed the strongest morphological changes. Laser number of shots and energy density are the main factors responsible for producing significant morphological changes in dentin surface. SEM results for all samples showed that there is a total elimination of smear layer, and there are some of open dentin tubules, but in all sample surfaces, clear traces of melting and re-crystallization that appears in the form of small debris and bubble can be seen. Using Nd:YAG laser with high energy density, at higher number of shots has led to both greater damage and more undesirable morphological changes. Interestingly this finding is in agreement with the findings of Moriyama et al [36]. By increasing the energy density, the results showed formation of well-defined crater edges with the existence of margins, debris and bubbles. The later result is in total agreement with the findings of Watanabe et al [37]. Lin et al. also observed cavities appearance [36]. Moreover, Lin et al also observed the globules (bubble) and debris formation inside the craters. They also observed the formation of fissures and melting traces not only inside the craters but also outside the craters. Increasing the energy density and the number of shots will lead to forming a deeper crater with fissures and melting surface [36]. Despite the fact that dentin has a low absorption coefficient in near infrared region, Nd:YAG laser (which emit light in the near infrared at 1064 nm) was able to damage dentin and forms craters in dentin surface. SEM results show a clear melting impact caused by local temperature rising during the photo-thermal interaction. Dentin tissue molecules absorb photons leading to the generating of heat that spreads in tissue. The absorbed energy depends on the molecule structure, wavelength, and energy densities. Since the tissue needs some time for the heat to propagate it, the ablation process depends on the tissue absorption coefficient
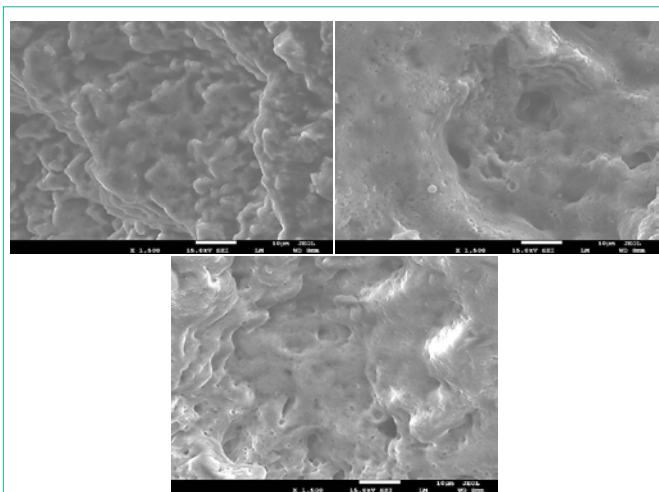
Figuer 13: Enamel surface after being irradiated with laser energy densities of 17.08,11.18, and 5.6 J/cm².

and the pulse duration. So, when pulse duration is approximately shorter than 100 ns, the ablation process begin at the end of the pulse and can continue for many hundreds of microseconds after the laser pulse finishes [36].

Enamel SEM result: Enamel surface was irradiated with five nanosecond Nd:YAG laser irradiation using energy densities of 17.08,11.18, and 5.6 J/cm². The FESEM image is shown in (Figure 13). Even with using a higher energy density than that used for dentin and the same number of shots, enamel does not show a deep crater like dentin. It is also difficult to obtain a homogeneous shape of the crater in enamel using low energies densities, so higher energy densities were used throughout the work of this article. This is due to the different composition between enamel and dentin owing to the fact that enamel tissue is more calcified than dentin. Enamel, was observed to be much harder than dentin, which is due to its different compositions. Interestingly, laser treatment produced a remarkable change of enamel rods. It altered their original shape size and arrangement. Thus, enamel rods took variable shapes; they became larger and acquired irregular arrangements. The melting and the following solidification process of the enamel produced a morphology characterized by columns and separated by voids. Samples, which were exposed to a high number of shots or a higher energy density, showed the strongest morphological changes. FESEM results showed a total elimination of smear layer exactly as dentin result. When using lower energy densities, it was possible to see the enamel rods. However, enamel rods completely disappear when using medium to
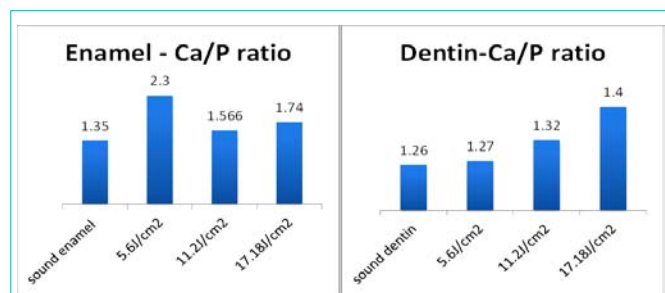
Figure 14: Enamel and dentin Atomic% Ca / P ratio.

high energy densities. By then, only molten surface were observable. The later results were in agreement with the findings of Rode et al [36]. The reason of the fissures appearance on enamel surface more than in dentin is due to sudden and fast changes in temperature, it causes damage in the enamel tight structure. Unlike dentin that contains pores which lead to the distribution of heat, enamel could not distribute the heat because it has unique structure which is completely different from dentin. To achieve greater ablation depth with minimal surface morphological alterations, energy density must not exceed 11.18 J/cm² [38].
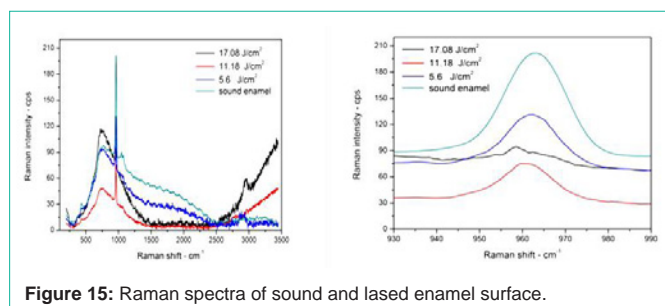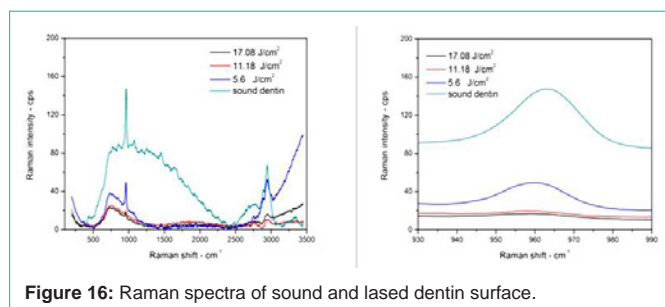
Spectroscopy analysis

In order to Study the chemical change, herein, two spectroscopic techniques were considered, EDS quantitative analysis, which give the changes in elements atomic percentage after laser irradiation, and IR spectrum. Micro Raman Spectroscopy analysis was used to determine the changes in bonds between atoms.

EDS result: In dentistry, it is very difficult to conduct true quantitative analysis. This is partly because of irradiated teeth samples being not flat. The second reason is that there is no standard reference for all types of samples like metallic, biological, etc. For these cases, usually the peaks in sample spectrum are compared with the peak of the pure element. However a semi-quantitative analysis can be conducted, if the following factors are taken into account: The SEM and EDS setup parameters such as applied voltage, magnification, spot size, etc. that must be fixed through experience. Since this work deals with a hydroxyapatite compound, which contains low atomic numbers elements, such as calcium-Ca, phosphorus-P, carbon-C and oxygen-O, long spectrum acquisition time was used in order to obtain a good signal to noise ratio with well-defined peaks and high number of counts. Even with these precautionary measures, the relative error in the calculations of approximately 10% or more if the concentration of certain elements is less than 5%must be taken into consideration [39]. Herne the focus is on increasing the carbon atomic percentage; because the excessive increase in carbon, atomic percentage may indicate the burning. Moreover, the changes in calcium and phosphorus atomic percentage were studied. Murray reported the Ca/P ratio in weight percentage for human teeth varied from 1.6 to 2.15 [40]. The percentage of calcium and phosphorus after laser irradiation are very important because it is affecting the Ca/P ratio. This ratio did not show a decrease after Nd:YAG laser irradiation as shown in (Figure 14). However, the increment of Ca/P ratio can improve the properties of tooth specifically enamel. The obtained results from the EDS semi quantitative analysis showed significant increase in Ca/P ratio for all irradiated dentin and enamel samples, especially at higher energy densities. With increased energy density, dentin showed a steady increase in the Ca/P ratio. As is evident from the Table 2, the atomic % of Ca and P both decrease compared to the non-irradiated sample, however the depletion of P is faster than Ca (as seen clearly in Figure 14) and therefore the ratio Ca/P increases. The increase in the case of dentin is gradual, whereas it increases initially to a high value and then shows a decrease and then gradual increase. The laser irradiation produces heat which results in evaporation of Ca and P, but since the vapor pressure of P is more than that of Ca, it depletes faster. The results obtained need more investigations to verify this hypothesis.

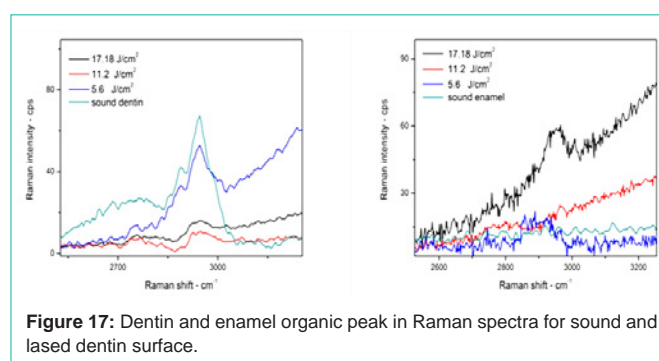**Table 2:** Elements atomic % before and after laser treatment.

	Energy density- (J/cm²)	C%	O%	P%	Ca%
Enamel	non irradiated	19.46	56.10	10.07	13.66
	5.6	48.92	40.83	3.02	6.96
	11.18	34.05	49.87	6.04	9.46
	17.08	55.88	31.56	4.45	7.75
Dentin	non irradiated	19.89	61.91	7.71	9.73
	5.6	45.16	46.32	3.43	4.39
	11.18	51.24	38.04	4.04	5.36
	17.08	56.33	35.96	3.03	4.26

Table 3: Phosphate Peak position and peak integrated areas.

Sample	Energy density (J/cm²)	Phosphate Peak position (cm⁻¹)	Integrated areas of peak
Dentin	Sound dentin	963.4	6978.4
	5.6	959.5	1992.5
	11.2	958.5	753.2
	17.08	958	730.3
Enamel	Sound enamel	963.4	7316.5
	5.6	962.4	5250
	11.2	959.6	2591.5
	17.08	958.6	4024.5

Figure 15: Raman spectra of sound and lased enamel surface.

Figure 16: Raman spectra of sound and lased dentin surface.

Figure 17: Dentin and enamel organic peak in Raman spectra for sound and lased dentin surface.

Micro Raman spectroscopy result: The most accurate method to study the impact of laser on materials molecules is the micro-Raman spectroscopy. It is a method that allows having information on the organic and inorganic materials of the tooth [41]. An IR spectrum consists of two major regions, the first region is above Raman shift of 1500cm⁻¹, there are absorption bands that can be assigned to individual functional groups, whereas, the second region below 1500cm⁻¹ contains many bands and characterizes the molecule as a whole. The bands within the fingerprint region, which arise from functional groups [41]. Raman spectra of sound and lased enamel surface are shown in (Figure 15). It is clear, there are very strong peaks at 960cm⁻¹, which belong to stretching vibration modes of phosphate included in the inorganic mineral crystalline hydroxyapatite, $Ca_{10}(PO_4)_6(OH)_2$. Normally phosphate peaks appear at Raman shift of 432, 585, 960, and 1044 cm⁻¹ [41]. Peaks above 1500cm⁻¹ are due to the vibration modes of organic components of NH (amide III), CH_3–CH_2 (amide I) groups. Organic peaks which are found at Raman shift of 1250, 1459 and 1663 cm⁻¹ can only be found in dentin [42]. As notices from (Figure 15 and Figure 16), the background of micro Raman spectra was higher in the irradiated dentin and enamel than in sound enamel and dentin. Moreover, the background in the spectra was increasing with energy density increment for both enamel and dentin. The background, mostly contributed by fluorescence, which

is lower as the binding is tighter. Therefore, the high background in the laser-irradiated surface suggests a breakage of the cross-linking in the structure [43]. The fluorescent intensity is usually much higher than the weak Raman signal in biological samples. Often there are two methodologies which have been used to detect weak Raman signals from biomaterials; surface-enhanced Raman scattering, and fluorescence background subtraction which is known as baseline correction [44]. In this reported work, baseline correction to reduce fluorescence background was used specifically in enamel sample at which a very clear fluorescence background in the region between 2600 to 3200cm⁻¹ can be seen. However, it was not possible to remove it even after using this method, which was more effective in dentin sample. Phosphate peak position and peak-integrated areas are shown in (Table 3).

From (Table 3) we notice that the peak position of v1 phosphate of all samples has a slight shift to the left, or to lower energy density, which means that binding becomes weaker. Dentin and enamel organic peak in Raman spectra for sound and lased dentin surface are shown in (Figure 17). In (Figure 17) there is a strong peak at 2940 cm⁻¹ with one small shoulder at 2840 cm⁻¹ which were identified in previous studies, generally assigned to stretching vibrations of C–H functional groups [45,46], and return to the CH_2 stretching vibration. This peak is mainly composed of three broad bands, centered at 2880, 2939 and 2985cm⁻¹ respectively. Peaks at 2939 cm⁻¹ and at 2985 cm⁻¹ can be attributed to CH_2 stretching vibrations in symmetric and asymmetric mode, respectively [42]. Following laser irradiation at energy density 5.6 J/cm², the organic materials peak intensity of 2940 cm⁻¹, C–H band decreased and became broader. The organic materials peak disappears completely when using energy density of 11.2 and 17.08 J/cm². The collagen peaks disappeared after Nd:YAG

laser irradiation on the dentin surfaces. This finding suggests that by increasing the laser energy, the more collagen binding was destroyed [43]. The most safe laser energy density to use was 5.6J/cm^2; it made the binding weaker, but still did not destroy the binding as was happening when energy densities of 11.2 and 17.08 J/cm^2 were used. It was observed those using laser energy densities of 11.2 and 17.08 J/cm^2 were not suitable to treat dentin because they have destroyed the organic material. This is due to the fact that dentin contains a high percentage of organic material primarily collagen [28]. Enamel is very different from dentin, the organic matrix peak intensity increases with increasing energy density. Specifically at 2840 cm^{-1}, laser treatment may cause thermal decomposition of the carbonated enamel apatite and the organic matters, which, despite being a minor composition, may play a significant role in inhibiting enamel diffusion and dissolution, and thus prevent enamel demineralization [45].

Conclusion

Results of this work concluded that dentin revealed lower ablation threshold than the ablation threshold for enamel. The crater depth measurements show that crater depth per pulse obtained by Nd:YAG laser in dental enamel and dentin are in the μm region. The measured ablation depth is enhanced by using number of consecutive pulses. Moreover, the morphology of processed cavities in dentin and enamel inspection showed superior tissue quality. Interestingly, we concluded that an appropriate set of laser parameters have led to surfaces with no evidence of melting, carbonization or micro-cracks. The surrounded ablated region of enamel and dentin showed thermal damage. Micro Raman spectra were effective in hard tissue ablation studies. Spectra showed that identified band at 960cm^{-1} (in both enamel and dentin) corresponding to the vibration modes of PO_4. The PO_4 band shifted towards the left with increased energy density for both enamel and dentin. This demonstrates that the band became weaker with increasing energy density. However, comparing between dentin and enamel PO_4 band at same laser parameters, dentin PO_4 band was more damaged in comparison with PO_4 band in enamel. Interestingly, the EDS quantitative analysis showed significant increase in the atomic percentage of carbon in tandem with an increase in laser energy density for enamel and dentin. This is attributed to thermal damage resulting from ablation. Unpresented EDS quantitative analysis showed increased in Ca/P ratio by increasing the laser energy density for enamel and dentin.

References

1. Verma SK, Maheshwari S, Singh RK, Chaudhari PK. Laser in dentistry: An innovative tool in modern dental practice. Nat J Maxillofac Surg. 2012; 3: 124-132.

2. White JM, Swift EJ. Lasers for use in Dentistry. Journal of Esthetic and Restorative Dentistry. 2005; 17: 60.

3. Fantarella, David, Larry K. The 9.3 μm CO_2 dental laser: Technical development and early clinical experiences. J Laser Dent. 2014; 22: 1.

4. Walsh LJ. The current status of laser applications in dentistry. Aust Dent J. 2003; 48: 146-155.

5. Toma S. Comparison of the Dynamic Response of a Tooth Between a High-Speed Drill and Dental Laser. University of California. 2012.

6. Kimura Y, Yonaga K, Yokoyama K, Kinoshita J, Ogata Y, Matsumoto K. Root surface temperature increase during Er:YAG Laser irradiation of root canals. J Endod. 2002; 28: 76-78.

7. Niemz MH. Laser-Tissue Interactions: Fundamentals and Applications. Springer. 2003.

8. Convissar RA. Principles and Practice of Laser Dentistry. Elsevier Health Sciences. 2010.

9. ADA Council on Scientific Affairs. Statement on Lasers in Dentistry. 2009.

10. Kim KS, Kim ME, Shin EJ. Irradiation time and ablation rate of enamel in contact and non-contact irradiation with Er:YAG laser. Photomed Laser Surg. 2005; 23: 216-218.

11. Neev J, Da Silva LB, Feit MD, Perry MD, Rubenchik AM, Stuart BC. Ultrashort Pulse Lasers for Hard Tissue Ablation. IEEE Journal of Selected Topics in Quantum Electronics. 1996; 2; 790-800.

12. Von Fraunhofer JA, Allen DJ. Thermal effects associated with the Nd/YAG dental laser. Angle Orthod. 1993; 63: 299-304.

13. Dederich DN, Bushick RD. Lasers in dentistry: Separating science from hype. J Am Dent Assoc. 2004; 135: 204-212.

14. Malik NA. Textbook of Oral and Maxillofacial Surgery. 3rd Edn. Jaypee Brothers Medical Publishers. 2012.

15. Chandra S, Chandra S, Chandra M, Chandra N, Chanrda G. Textbook of Dental and Oral Histology and Embryology with MCQs. 1st Edn. Jaypee Brothers Medical Publishers. 2007.

16. Rajendran R, Sivapathasundharam B. Shafer'S Textbook of Oral Pathology. 6th Edn. Elsevier. 2009.

17. Cernavin I, Hogan SP. The effects of the Nd:Y AG laser on amalgan dental restorative material. Australian Dental Journal. 1999; 44: 98-102.

18. Steiner R, Raulin C, Karsai S. Laser and IPL Technology in Dermatology and Aesthetic Medicine.1st Edition. Springer. 2011.

19. Welch AJ, van Gemert MJC. Optical-Thermal Response of Laser-Irradiated Tissue. 2nd Edition. Springer. 2011.

20. Jacques SL. Laser-tissue Interaction. SPIE. 2003.

21. Brodie LM. Welding of Skin Using Nd:YAG Laser with Bipolar Contact Applicators. University of Southern Queensland. 2003.

22. Gamaly EG, Rode AV, Luther-Davies B. Pulsed Laser Deposition of Thin Films: Applications-Led Growth of Functional Materials. John Wiley & Sons Inc. 2006.

23. Russo RE, Mao XL, Yoo JH, Gonzalez JJ. Laser-Induced Breakdown Spectroscopy. Elsevier. 2007.

24. Lee H. Pulsed Laser-Induced Material Ablation and its Clinical Applications. The University of Texas. 2003.

25. Yoo JH, Jeong SH, Greif R, Russo RE. Explosive change in crater properties during high power nanosecond laser ablation of silicon. Journal of Applied Physics. 2000; 88: 1638-1649.

26. Batani D. Laser Ablation and Laser Induced Plasmas for Nanomachining and Material Analysis. Springer. 2008.

27. Nanci A. Ten Cate's Oral Histology. 8th Edition. Elsevier. 2007.

28. Eason RW, May-Smith TC, Sloyan KA, Gazia R, Darby MSB, Sposito A, et al. Multi-beam pulsed laser deposition for advanced thin-film optical waveguides. Journal of Physics D Applied Physics. 2014.

29. Harilal SS, Miloshevsky GV, Diwakar PK, Lahaye NL, Hassanein A. Experimental and computational study of complex shockwave dynamics in laser ablation plumes in argon atmosphere. Physics of Plasmas. 2012.

30. Gaudiuso R, Dell'Aglio M, Pascale OD, Senesi GS, Giacomo AD. Laser Induced Breakdown Spectroscopy for Elemental Analysis in Environmental, Cultural Heritage and Space Applications: A Review of Methods and Results. Sensors(Basel). 2010; 10: 7434-7468.

31. Al-Hadeethi Y, Al-Jedani S, Razvi MAN, Saeed A, Abdel-Daiem AM, Ansari MS, et al. Data Fitting to Study Ablated Hard Dental Tissues by Nanosecond Laser Irradiation. PLoS One. 2016.

32. Avery JK, Steele PF, Avery N. Oral Development and Histology. 3rd Edn. Thieme. 2001.

33. Lin S, Liu Q, Peng Q, Lin M, Zhan Z, Zhang X. The ablation threshold of Er:YAG laser and Er,Cr:YSGG laser in dental dentin. Scientific Research and Essays. 2010; 5: 2128-2135.

34. Siniaeva ML, Siniavsky MN, Pashinin VP, Mamedov AA, Konov VI, Kononenko VV. Laser Ablation of dental materials using a microsecond Nd: YAG laser. Laser Physics. 2009; 19: 1056-1060.

35. de Souza MR, Watanabe IS, Azevedo LH, Tanji EY. Morphological Alterations of the Surfaces of Enamel and Dentin of Deciduous Teeth Irradiated with Nd:YAG, CO_2 and Diode Lasers. Int J Morphol. 2009; 27: 441-446.

36. Lizarelli RFZ, Kurachi C, Misoguti L, Bagnato VS. A Comparative Study of Nanosecond and Picosecond Laser Ablation in Enamel: Morphological Aspects. Journal of Clinical Laser Medicine and Surgery. 2000; 18: 151-157.

37. Corona SAM, Souza-Gabriel AE, Chinelatti MA, Pecora JD, Borsatto MC, Palma-Dibb RG. Influence of energy and pulse repetition rate of Er:YAG laser on enamel ablation ability and morphological analysis of the laser-irradiated surface. Journal of Biomedical Materials Research. 2008; 84: 569-575.

38. Contreras-Bulnes R, Olea-Mejia OF, Rodriguez-Vilchis LE, Scougall-Vilchis RJ, Centeno-Pedraza C. Structural Changes on Human Dental Enamel Treated with Er:YAG, CO_2 Lasers and Remineralizing Solution: EDS Analysis. InTech. 2012.

39. Rey C, Combes C, Drouet C, Glimcher MJ. Bone mineral: update on chemical composition and structure. Osteoporos Int. 2009; 20: 1013-1021.

40. Socrates G. Infrared and Raman Characteristic Group Frequencies: Tables and Charts, 3rd Edn. Wiley. 2004.

41. Camerlingo C, Lepore M, Gaeta GM, Riccio R, Riccio C, De Rosa A, et al. Er:YAG laser treatments on dentine surface: micro-Raman spectroscopy and SEM analysis. J Dent. 2004; 32: 399-405.

42. Yamada MK, Uo M, Ohkawa S, Akasaka T, Watari F. Three-dimensional topographic scanning electron microscope and Raman spectroscopic analyses of the irradiation effect on teeth by Nd:YAG, Er: YAG, and CO_2 Lasers. Journal of Biomedical Materials Research. 2004.

43. MarquesMP, de Carvalho LAEB, Haris PI. Spectroscopy of Biological Molecules Proceedings from the 14th European Conference on the Spectroscopy of Biological Molecules. 2011. IOS Press. 2013.

44. Liu Y, Hsu CY. Laser-induced compositional changes on enamel: A FT-Raman study. Journal of Dentistry. 2007; 35: 226-230.

45. Kirchner MT, Edwards HGM, Lucy D, Pollard AM. Ancient and Modern Specimens of Human Teeth: a Fourier Transform Raman Spectroscopic Study. Journal of Raman Spectroscopy. 1997; 28: 171-178.